Journal of Chromatography, 125 (1976) 203–215

CHROM. 9532

RADIOCHEMICAL AND ISOTOPE SEPARATIONS BY HIGH-EFFICIENCY LIQUID–LIQUID CHROMATOGRAPHY*

E. P. HORWITZ, W. H. DELPHIN, C. A. A. BLOOMQUIST and G. F. VANDEGRIFT
Chemistry Division, Argonne National Laboratory, 9700 South Cass Avenue, Argonne, Ill. 60439 (U.S.A.)

SUMMARY

A very-high-efficiency liquid–liquid chromatographic (LLC) system based on 5- and 20-μm diameter porous silica microspheres was used to effect radiochemical separations of metal ions that required very large decontamination factors and/or high speeds. The stationary phase was 25–30% (w/w) of di(2-ethylhexyl) orthophosphoric acid (HDEHP) in dodecane. Nitric acid was used as the mobile phase. The mass transfer coefficient term, C, was determined from height equivalent to a theoretical plate *vs.* interstitial linear velocity data for the elution of Ca^{2+} and compared with values calculated from the interfacial mass transfer coefficients measured in the corresponding liquid–liquid extraction system. The HDEHP high-efficiency LLC system was also investigated for possible use in enriching the naturally occurring isotopes of calcium. Isotopic exchange constants for ^{40}Ca or ^{42}Ca and ^{48}Ca were measured chromatographically as a function of temperature. The enrichment of calcium isotopes was attempted on coupled columns at low flow velocities.

INTRODUCTION

Liquid–liquid chromatography (LLC) applied to the separation of metal ions utilizes selective organic extractants as the stationary phase and aqueous solutions as the mobile phase. This form of LLC, which is frequently referred to as extraction chromatography, differs considerably from the partition chromatography normally carried out on organic compounds. The differences arise because in the extraction of metal ions, either by LLC or liquid–liquid extraction (LLE), an initially ionic solute is transferred from an aqueous to an organic phase, in which it is present as some type of neutral complex. This type of reaction involves rather complex interactions and large chemical changes. On the other hand, the usual mode of partition chromatography involves rather weak interactions and associations and, therefore, little if any chemical change.

LLC is particularly advantageous for radiochemical separations because it

* Based on work performed under the auspices of the U.S. Energy Research and Development Administration.

combines the selective characteristics of the organic compounds used in LLE with the resolution features of the chromatographic process. The most useful, and therefore the most popular, stationary phases for radiochemical LLC separations are the dialkyl and trialkyl esters of phosphoric acid and the tertiary and quaternary ammonium salts. These extractants show large selectivities for a wide variety of metal ions and have, in general, favorable kinetic properties. Column efficiencies in radiochemical LLC separations, although somewhat low initially[1], have been improved greatly during the last few years owing to the use of smaller and more uniform practicle size supports, to improved packing techniques, and to the use of the new chromatographic supports now available[2–5].

Recent work by three of us[6] describes a very-high-efficiency radiochemical separation system based on the use of 5-μm-diameter porous silica microspheres (PSM) as the inert support. The well characterized extractant di(2-ethylhexyl) orthophosphoric acid (HDEHP) in dodecane was used as the stationary phase. This paper describes a continuation of these studies using the same high-efficiency LLC system. The objectives in this investigation are threefold: First, to determine the applicability of interfacial transfer coefficients measured in an LLE system for calculating the chromatographic mass transfer term, C, in the corresponding high-efficiency LLC system; second, to apply the high-efficiency LLC system based on PSM support to several important radiochemical separation problems; and third, to extend high-efficiency LLC to the problem of enriching naturally occurring stable isotopes. The naturally occurring isotopes of calcium were selected for the latter study because of the excellent column performance obtainable for the elution of Ca^{2+}. Enriched ^{44}Ca, ^{46}Ca, and ^{48}Ca are also of some interest as non-radioactive tracers.

EXPERIMENTAL

Column material

The porous silica microspherical supports Zorbax-SIL (5-μm particle size) and Spherisorb S20W (20-μm particle size) were obtained from DuPont Instrument Products Division (Wilmington, Del., U.S.A.) and Spectra-Physics, Autolab Division (Santa Clara, Calif., U.S.A.), respectively. These supports were made hydrophobic, coated with stationary phase, and wetted prior to slurry packing using the procedures described previously[6].

Reagents, radioactive and stable isotopes

All acid solutions were prepared using Ultrex-grade acids (J. T. Baker, Phillipsburg, N.J., U.S.A.) and ultra-pure water obtained from a Milli-Q2 system water purifier (Millipore Corp., Bedford, Mass., U.S.A.).

The sources and purifications of all radioactive materials were described previously[7]. The stable calcium isotopes, ^{42}Ca, ^{44}Ca, and ^{48}Ca, with isotopic purities in the range of 95–99% were obtained (as carbonates) from the Isotopes Development Center, Oak Ridge National Laboratory (Oak Ridge, Tenn., U.S.A.).

Apparatus and columns for radiochemical experiments

The LLC apparatus, column packing procedure, and column run techniques used for the high-efficiency radiochemical separations were described in a previous

paper[6]. In this equipment liquid contacts only glass and PTFE; thus hydrohalic acids as well as nitric acid can be used as eluents. The system will withstand a maximum pressure of 500 p.s.i.

Apparatus for isotope separation experiments

The isotope separation experiments were carried out using both the low-pressure glass–PTFE system referred to above and a Spectra-Physics Model 3500B high-pressure liquid chromatograph (Spectra-Physics, Autolab Division), which was equipped with steel columns and a high-pressure loop injection valve. Liquid contacts only 316 stainless steel. Columns were 25 and 50 cm in length and 3 mm in internal diameter and were fitted with a Kel-F bed support containing a 2-μm stainless-steel frit. A 1-μm Nuclepore membrane filter was placed over the bed support at the bottom of the column. All stainless-steel end fittings (Swagelok) had minimum dead volume and clean flow-through patterns. Thermostating of columns was achieved using a Spectra-Physics Type SSJ jacket and a constant-temperature circulator (Haake, Rochelle Park, N.J., U.S.A.). A U-Cool auxiliary cooling system (Neslab, Portsmouth, N.H., U.S.A.) in series with a Haake circulator was used to achieve thermostating at 9–10°.

All columns were high-pressure slurry packed using a 15 cm × 10 mm I.D. steel column as a packing reservoir. Non-aggregated dispersions of column material in 0.1 *M* nitric acid were prepared as described previously[6]. After packing, a 1-μm Nuclepore membrane filter was placed over the top of the bed. The column was then sealed using an end fitting containing a Kel-F bed support with the frit removed. Columns were coupled together using a 4-in. length of 0.019-in.-I.D. tubing with Swagelok end fittings.

Isotopic separation factor measurements

Separation factors, α, (defined as the ratio of the heavy to light isotope in the organic phase divided by the ratio of the heavy to light isotope in the solution phase) were determined using the equation of Glueckauf[8]:

$$\ln R = -N\varepsilon \frac{\bar{v} - v}{\sqrt{\bar{v} \cdot v}} \qquad (1)$$

where R is the local isotopic enrichment at point v of the elution curve, N is the number of theoretical plates, $\varepsilon = \alpha - 1$, and $\bar{v}$ is the peak maximum of the elution curve. (The local enrichment, R, is defined as the ratio of the heavy to light isotope in the eluate fraction v divided by the ratio of the heavy to light isotope in the feed.)

Column runs performed for the purpose of measuring α were usually carried out using 25-cm-long MB-3 glass columns and the low-pressure (500 p.s.i.) LLC system[6]. A mixture of ^{42}Ca (or ^{40}Ca) and ^{48}Ca, in one-to-one ratio and totalling approximately 5–10 μg, and *ca.* 10^5–10^6 cpm of ^{45}Ca was loaded on a column from *ca.* 100–200 μl of 10^{-3} *M* nitric acid. After loading, the column was eluted with 0.044 *M* nitric acid (capacity ratio, $k' = 6$) and the drop number of eluate was counted electronically. The calcium elution band was collected in fractions consisting of single drops on clean stainless-steel plates (15/16 in. in diameter and 0.003 in. thick). After evaporating the drops to dryness under a heat lamp, the plates were counted for ^{45}Ca

using a proportional end-window beta counter with an automatic sample changer and a printer. The number of theoretical plates was calculated from the plotted elution curve[7]. Individual fractions of the calcium elution band were selected for mass spectrometric analysis. The calcium in these fractions was recovered from the stainless-steel plates by leaching with 10–20 μl of 10^{-3} *M* nitric acid and transferring the remaining solution into a 400-μl Eppendorf micro test tube (Bio-Rad Labs., Richmond, Calif., U.S.A.). This procedure was repeated to improve recovery of the residue. A Rainin digital Pipetman with disposable polypropylene pipet tips (Rainin, Boston, Mass., U.S.A.) was used to transfer acid and leached samples. The disposable pipet tips and micro test tubes were thoroughly cleaned by soaking overnight in 0.1 *M* nitric acid followed by multiple rinsings with ultra-pure water. Mass spectrometric analysis was performed directly on the leached solutions, which contained the recovered calcium isotopes in 10^{-3} *M* nitric acid, and on a sample of the feed solution.

Since these experiments involved very minute quantities of the heavy calcium isotope, ^{48}Ca, there were considerable problems in obtaining accurate ^{48}Ca/^{40}Ca ratios owing to adventitious contamination of samples with natural calcium. Although some very good data were obtained on the α for ^{48}Ca/^{40}Ca, better data were obtained using a mixture of ^{42}Ca and ^{48}Ca since both of these isotopes have abundances of less than 1% in natural calcium.

Isotopic enrichment experiments

Column runs performed for the purpose of enriching ^{48}Ca were carried out using the Spectra-Physics high-pressure liquid chromatograph with steel columns. The procedure was essentially the same as that used to measure α. Radioactive calcium (^{45}Ca) was always used to detect the $^{40-48}$Ca band. Eluate fractions were recovered and assayed radiometrically and mass spectrometrically using the same procedure as described above.

RESULTS AND DISCUSSION

Extraction mechanism and interface structure

All high-efficiency LLC systems require rapid interfacial mass transfer of a solute between the mobile and stationary phases[9]. In order to investigate further the magnitude of the mass transfer term in LLC and to elucidate the extraction mechanism, Vandegrift and Horwitz[10] measured the interfacial transfer coefficients of Ca^{2+} in the LLE system, dilute nitric acid–HDEHP in dodecane. The interfacial transfer coefficients, which were measured across a quiescent interface, are defined by the following equation:

$$-\frac{dc_{org}}{dt} = \frac{A_I}{v_{org}}(k_{oa}\,c_{org} - k_{ao}\,c_{aq}) \qquad (2)$$

where the term on the left is the rate of decrease of solute in the organic phase (in moles·cm^{-3}·sec^{-1}), A_I is the interfacial area (in cm^2), v_{org} is the volume of organic phase (in cm^3), k_{oa} and k_{ao} are the interfacial transfer coefficients (in cm/sec) for mass transfer from the organic to aqueous phase and aqueous to organic phase, respectively, and c_{org} and c_{aq} are the concentrations (in moles/cm^3) of solute in the organic

and aqueous phases, respectively. The terms k_{oa} and k_{ao} are not simple constants but are complicated functions of the various individual rate processes.

Based on extensive k_{oa} and k_{ao} data as functions of a variety of experimental conditions, the following mechanism for the LLE of Ca^{2+} by HDEHP was postulated[10]:

$$Ca^{2+}_{(aq)} + (HDEHP)_{2(I)} \underset{k_{-1}}{\overset{k_1}{\rightleftharpoons}} Ca(DEHP)_{2(I)} + 2\,H^{+}_{(aq)} \tag{3}$$

$$Ca(DEHP)_{2(I)} + 2\,(HDEHP)_{2(org)} \underset{k_2}{\overset{k_{-2}}{\rightleftharpoons}} Ca(DEHP)_2 \cdot 4\,(HDEHP)_{(org)} \tag{4}$$

where (aq), (I), and (org) refer to the aqueous phase, interface, and organic phase, respectively. The negative sign in the rate constants indicates that the calcium ion is moving away from the interface, either towards the bulk aqueous or bulk organic phase; conversely, the positive sign indicates that calcium ion is moving toward the interface. The significant feature of this mechanism is that the Ca^{2+} first forms a neutral interfacial complex with a HDEHP dimer. This interfacial complex then reacts with additional HDEHP dimers to form some type of HDEHP solvated species of unknown structure. Since HDEHP is more interface active than the $Ca(DEHP)_2$ complex, the extractant molecules involved in the interfacial reaction are replaced by bulk extractant (E), thus completing the cycle.

The relationship between k_{oa} and k_{ao} and the various rate constants in eqns. 3 and 4 are shown below[10]:

$$k_{oa} = \frac{k_{-1}\,[H^+]^2 \cdot k_2}{k_{-1}\,[H^+]^2 + k_{-2}\,[E]^2_{org}} \tag{5}$$

$$k_{ao} = \frac{k_1\,[E]_I \cdot k_{-2}\,[E]^2_{org}}{k_{-1}\,[H^+]^2 + k_{-2}\,[E]^2_{org}} \tag{6}$$

The K_d, which is k_{ao}/k_{oa}, is given then by the following equation:

$$K_d = \frac{k_1\,[E]_I \cdot k_{-2}\,[E]^2_{org}}{k_{-1}\,[H^+]^2 \cdot k_2} \tag{7}$$

Using the above results, together with interfacial surface tension measurements[10], a simplified picture can be drawn of the interfacial structure of HDEHP. This is shown in Fig. 1. The significant feature of this figure is that the HDEHP dimer in the bulk phase is partly opened at the interface with the hydrophilic portion oriented towards and hydrogen bonded to a water layer. The resultant monolayer resembles a two-dimensional polymer network of HDEHP molecules hydrogen bonded to a structured water layer. Above the monolayer is a secondary layer of HDEHP dimers and a few trimers (in the concentrated half of the drawing) with their hydrophobic portions oriented towards and adjacent to the alkyl groups of the first monolayer. The phosphoric acid groups directed into the water layer are the radicals

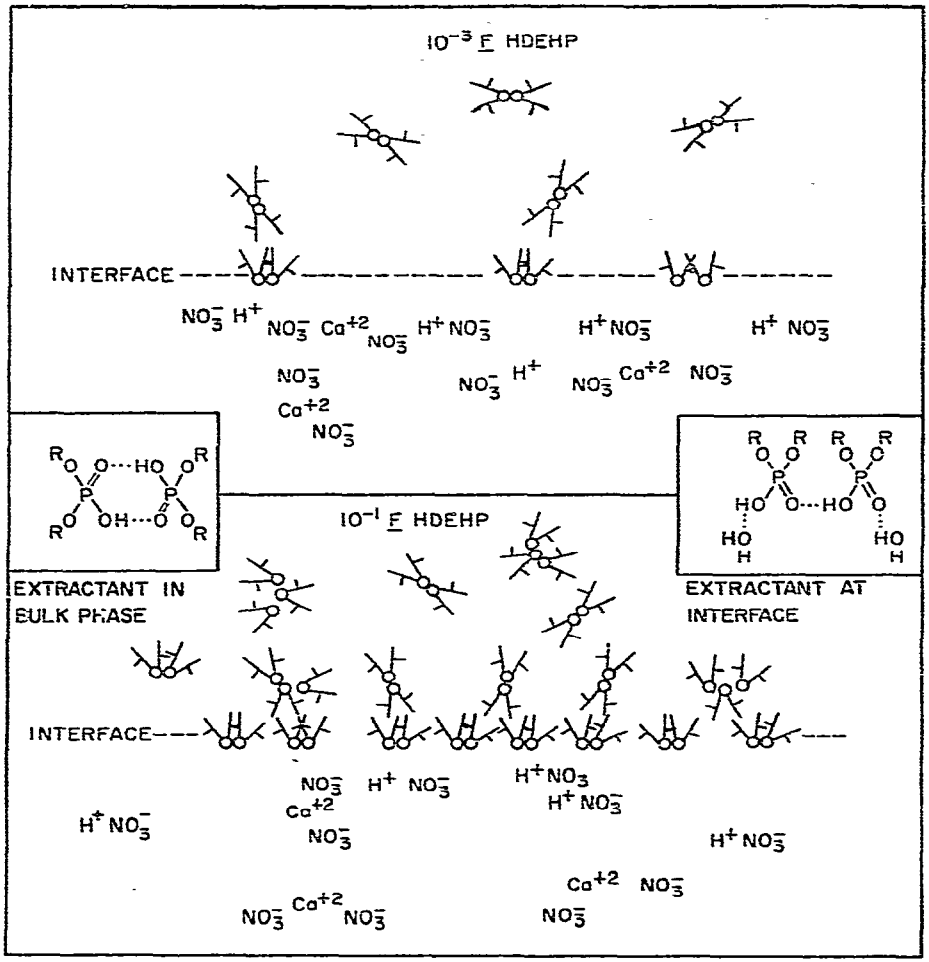

Fig. 1. Simplified picture of interface and bulk organic phase structure.

that are involved in the initial stages of dehydration and chelation of the calcium ion to form a neutral interfacial complex. It is probable that the formation of a neutral complex in the interface by these HDEHP molecules is a necessary condition for the rapid mass transfer of a given metal ion from the aqueous to the organic phase. Therefore, the surface activity of HDEHP and the resultant interfacial structure is at least partly responsible for the favorable kinetic features of this extractant.

Relationship between LLE and LLC rate constants

Assuming the same interfacial transfer coefficients and rate constants that were derived and measured for the LLE system are also valid in the corresponding LLC system, then the K_d's in the two systems should be the same. Fig. 2 shows the K_d's as a function of HNO_3 concentration, as measured by LLE and LLC. Two different pore size PSM supports were used in the LLC experiments, namely, commercial Zorbax-SIL containing 75-Å-diameter pores and a wide-pore PSM support

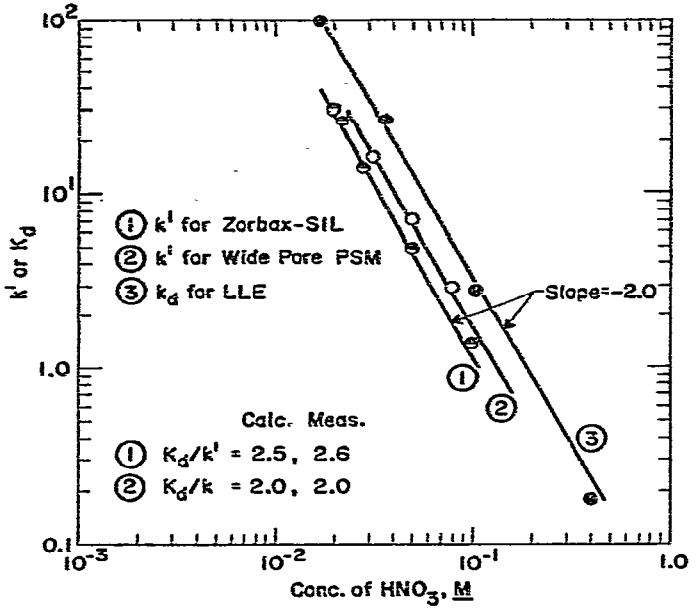

Fig. 2. Acid dependency of k' (LLC) and K_d (LLE) for the elution and extraction of Ca(II). 1.5 F HDEHP in dodecane is the stationary and organic phases. $T = 25°$. Liquid loading: (1) 25% (w/w); (2) 22% (w/w). Column bed density: (1) 0.67 g/ml; (2) 0.87 g/ml.

containing 350-Å-diameter pores. The ratio of the K_d (from LLE) to k' (from LLC) should equal the calculated v_m/v_s, which is shown in Fig. 2 to be the case for both pore sizes. (The volume of stationary phase, v_s, was calculated from its weight percent on the support, its density (0.854 g/ml), and the column bed density, whereas v_m was taken as 0.49 times the bed volume.) In order to apply the interfacial transfer coefficient k_{oa} to a chromatographic system, the ratio of the interfacial area to the volume of stationary phase, A_I/v_s, must be calculated. The product $k_{oa} \cdot A_I/v_s$ is the first-order rate constant, k_{sm} (in sec^{-1}), for the mass transfer of calcium from the stationary to the mobile phase (see eqn. 2 and ref. 9).

Calculation of the interfacial area in the case of a 5-μm PSM support was accomplished by two different methods. The first and simplest approach was to calculate the ratio of the surface area to the volume of a sphere, which is equal to $3/r$ (where $r = 2.5 \cdot 10^{-4}$ cm). Dividing by 0.36 (fraction of the volume of spheres occupied by liquid) and multiplying by v_s (0.20 ml/1 ml bed volume) gave the surface area of a 1-ml column packed with 5-μm-diameter particles. The assumption was then made that one half of the surface contains pore openings and that these pores are filled with liquid which forms a concave hemispherical interface. Using this assumption, $A_I = 6.8 \cdot 10^3$ cm^2/ml of bed volume and $A_I/v_s = 3.4 \cdot 10^4$ cm^{-1}. This value is probably low because the pore openings of Zorbax-SIL do not have a spherical shape as assumed in the above calculation but more closely resemble four- and six-cusped hypocycloids. The hypocycloid-shaped pore would in effect produce a larger liquid–liquid interface.

The second approach is to calculate the surface area of the support remaining after filling the available pore space with liquid. This is estimated to be *ca.* 5% of the

350 m^2/g of total surface area (B.E.T.). Assuming that *ca.* 25% of the remaining surface is liquid interface, $A_I = 2.2 \cdot 10^4$ cm^2/ml of bed volume and $A_I/v_s = 1.1 \cdot 10^5$ cm^{-1}. The basis of this assumption is that the surface of Zorbax-SIL is botyroidal rather than smooth, which has the effect of increasing the surface area not filled with or in contact with liquid.

The two approaches give approximately similar values, with perhaps the mean value of $A_I/v_s = 6.1 \cdot 10^4$ cm^{-1} as the best approximation. Another value of A_I/v_s can be obtained using the empirical formula, $S\sqrt{Z} = 750$ (ref. 11), where S = the surface area per unit volume in cm^{-1} and Z = the screen opening in cm required to pass 80% of the particles (taken as $5 \cdot 10^{-4}$ cm in this case). Using the same refinements and assumptions as in the first calculation, $A_I/v_s = 9.3 \cdot 10^4$ cm^{-1}, which is well within a factor of two of the calculated mean value.

The k_{oa} values used in the calculation of k_{sm} were determined from the K_d at the $[H^+]$ of the mobile phase and from k_{ao} values which were corrected to an infinite stirring rate. This correction was necessary because it was found in the LLE study[10] that the exact values of k_{oa} and k_{ao} at a given $[H^+]$, [E], and T(°C) were a function of the stirring rate of the aqueous, but not organic, phase. This phenomenon was explained by postulating the existence of a structured "ice-like" water layer at the interface, the thickness of which depends on temperature and stirring rate. The justification for extrapolating k_{ao} to an infinite stirring rate is that the large increase in A_I/v_{org} ($>10^6$) and the high flow velocities in going from LLE to LLC would substantially reduce the thickness of the structured water layer. Thus, the conditions in LLC at high v (>6 cm/min) would be equivalent to an infinite stirring rate in LLE.

Table I tabulates the individual interfacial transfer coefficients (taken from ref. 10) and the first-order rate constants for the LLC system. The high and low value of A_I/v_s, as well as the mean, were used to calculate the k_{sm}.

Calculated and experimental mass transfer term, C

Using the high, low, and mean values of k_{sm} shown in Table I and $k' = 14$, the mass transfer term, C, was calculated using the equation derived by Giddings from the generalized nonequilibrium theory[12]:

$$C = \frac{2k'}{(1 + k')^2} \cdot \frac{1}{k_{sm}} \tag{8}$$

TABLE I

INTERFACIAL TRANSFER COEFFICIENTS AND FIRST-ORDER RATE CONSTANTS

Elution of Ca^{2+} with dilute nitric acid, $K_d = 35$, $v_m/v_s = 2.5$; 25% (w/w) of 1.5 *F* HDEHP in dodecane on 5-μm Zorbax-SIL.

T (°C)	H^+	k_{ao}* (cm/sec)	k_{oa} (cm/sec)	k_{sm}** (sec^{-1})	k_{sm}*** (sec^{-1})
10	0.036	$9.8 \cdot 10^{-4}$	$2.8 \cdot 10^{-5}$	$9.5 \cdot 10^{-1}$–3.1	1.7
25	0.029	$2.7 \cdot 10^{-3}$	$7.7 \cdot 10^{-5}$	2.6–8.5	4.7
50	0.019	$6.3 \cdot 10^{-3}$	$1.8 \cdot 10^{-4}$	6.1–20	11

* Taken from ref. 10.

** $A_I/v_s = 3.4 \cdot 10^4$ to $1.1 \cdot 10^5$ cm^{-1}.

*** $A_I/v_s = 6.1 \cdot 10^4$ cm^{-1}.

This equation is equivalent to the simple one-site adsorption equation where k_{sm} is replaced by the desorption rate constant. An equation equivalent to eqn. 8 can also be used to calculate the mass transfer term:

$$C = 2\left(\frac{k'}{1+k'}\right)^2 \cdot \frac{1}{k_{ms}} \tag{9}$$

where $k_{ms} = k_{ao} \cdot A_I / v_m$ and $v_m / v_s = K_d / k'$.

The experimental values of C were determined from the plate height (H) *vs.* v curves shown in Fig. 3. The simple relationship, $H = A + C\,v$, where v is the interstitial linear velocity in cm/sec, was used to determine the slope, C, above 5 cm/min. (Preliminary studies showed that diffusion in the stationary phase was not a major contributor; *i.e.*, $<10\%$, to band spreading.) The experimental and calculated mass transfer term, C, in milliseconds, is shown in Table II.

The agreement between the experimental and calculated C term is excellent, especially in view of the approximations used in calculating A_I and the extrapolation of k_{ao} to an infinite stirring rate. These results confirm, to a good approximation, that the same rate limiting steps in LLE also apply to LLC, under the right circumstances of pore size and liquid loading. Additional evidence for the similarity of the two systems was obtained by comparing the calculated and experimental H *vs.* k' function (or H *vs.* acidity, since $k' \propto 1/[H^+]^2$) at $v = 13$ cm/min. Both the experimental and calculated data showed no substantial capacity factor effect since k_{sm} decreases as k' increases.

These conclusions differ from the results reported by Nolte *et al.*[15], who

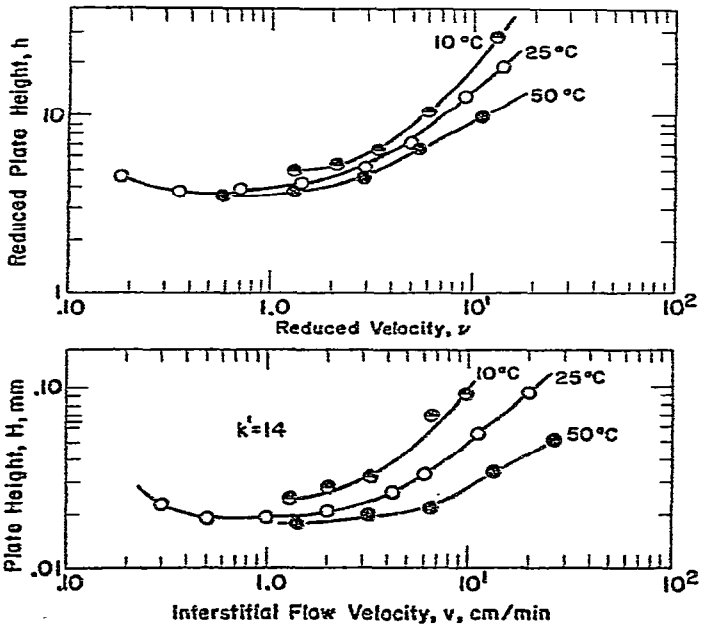

Fig. 3. H *vs.* v and h *vs.* v at 50, 25, and 10°. Elution of Ca^{2+} with dilute nitric acid from 25% (w/w) of 1.5 *F* HDEHP in dodecane on 5-μm Zorbax-SIL.

TABLE II

EXPERIMENTAL AND CALCULATED MASS TRANSFER COEFFICIENT, C

Elution of Ca^{2+} with dilute nitric acid. $k' = 14$; 25% (w/w) of 1.5 F HDEHP in dodecane on 5-μm Zorbax-SIL.

T (°C)	C (msec)		
	Experimental	*Calculated**	*Calculated***
10	57 ± 11	130–40	73
25	26 ± 3	48–15	26
50	8.9 ± 0.9	20– 6.3	11

* Calculated A_t/v_s range = $3.4 \cdot 10^4$ to $1.1 \cdot 10^5$ cm^{-1}.
** Mean $A_t/v_s = 6.1 \cdot 10^4$ cm^{-1}.

showed that pore diameters less than 300 Å in silica gel did influence both the rate of mass transfer and the distribution ratio of the europium using HDEHP stationary phase. The explanation for this disparity may lie in the difference in the internal structure of the 56-μm silica gel compared with the 5-μm PSM material, as well as in the presence of the large stagnant aqueous phase in 10% (w/w) loaded support. The mass transfer mechanism proposed for Ca^{2+} also differs from that proposed by Specht *et al.*[14] for Eu^{3+} using 10% (w/w) HDEHP on 56-μm silica gel. In this case, we do not feel that aqueous phase complexing of metal ions by dissolved HDEHP is a significant process. The data in ref. 10 for Ca^{2+} are inconsistent with any aqueous phase complexing.

Applications of the high-efficiency LLC system to radiochemical problems

Although many characteristics of the achievement of separation by LC are similar regardless of the type of solute, radiochemical separations usually place somewhat different requirements on the chromatographic system. This is particularly true of preparative radiochemical separations, which is the objective in the majority of cases. Table III outlines some of the characteristics of LLC radiochemical separations. Numbers one and two are due to the types of chemical reactions involved as described above. Complexing and chelation reactions usually show large differences in metal ions owing to electronic and molecular structure effects. These same chemical reactions are likely to be rate limiting and contribute to band spreading. This effect

TABLE III

CHARACTERISTICS OF LLC RADIOCHEMICAL SEPARATIONS

No.	*Parameter*	*Comment*
1	Separation factors	Usually larger than in LLC separations involving organic compounds
2	Column efficiencies	Usually lower (fewer plates/column length) than LLC systems used to resolve organic compounds
3	Sample size	A few atoms to many grams
4	Speed	High speed sometimes required because of short half-lifes or to minimize radiation damage
5	Decontamination factors	Many orders of magnitude are usually required, *e.g.*, 10^4–10^{15}

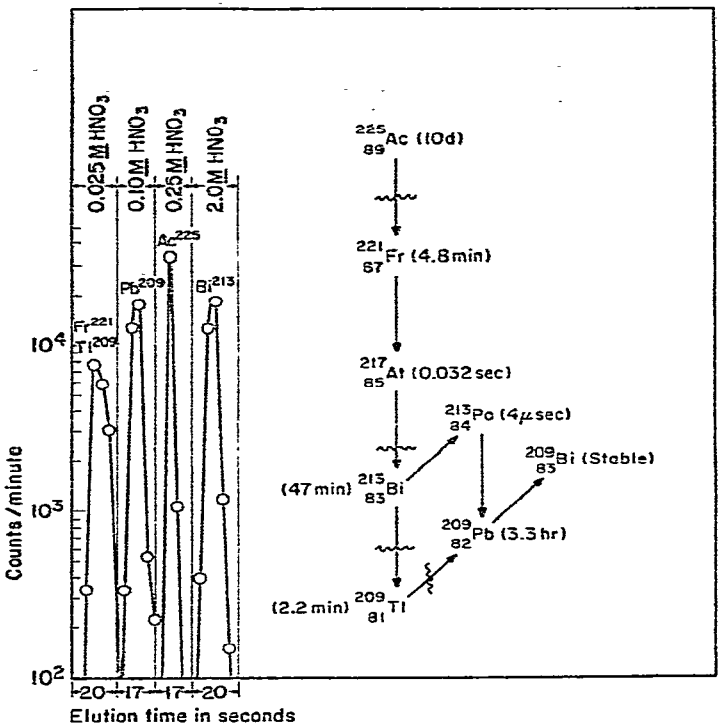

Fig. 4. High-speed separation of ^{225}Ac and daughter nuclides. Column bed = 1 cm × 2 mm I.D.; T = 50°; v = 17 cm/min. Column material = 30% (w/w) of 1.5 *F* HDEHP in dodecane on 5-μm Zorbax-SIL.

can be partly obviated by increasing column temperature, as shown in Fig. 3 and Table II. Numbers 3 and 4 require no additional comment. Number 5, decontamination factors, places the greatest demand on the LLC system. Nuclear properties, such as half-life or cross section, differ by many orders of magnitude and frequently one part per million or billion (10^9) of an impurity or product isotope must be separated. High-performance chromatography is essential in order to meet these requirements efficiently.

Three examples of the application of high-performance LLC are given below. Each example demonstrates the different requirements that are placed on chromatographic performance.

High-speed separation of $^{225}_{89}$ Ac and daughters. Fig. 4 shows the high-speed separation of ^{225}Ac and its daughters (in secular equilibrium), ^{221}Fr, ^{213}Bi, ^{209}Tl, and ^{209}Pb, in approximately 1 min. The large number of plates obtainable using the high-performance LLC system (200–300 at v = 17 cm/min), in addition to its large selectivity, made it possible to achieve this separation on a 1-cm-long column. Using very short columns has several advantages, *i.e.*, separation time is less, the nuclides of interest are obtained in a smaller volume, and fewer problems are encountered with packing and preconditioning the column. The large separation factors permit the sequential elution of the individual nuclides by step changing the acidity, which makes the resolution of the mixture even easier.

There are many applications of this type of radiochemical separation where the emphasis is on speed and not on decontamination factor. High-performance LLC using HDEHP or tricaprylmethyl ammonium chloride, nitrate, or thiocyanate as stationary phases on 5-μm PSM support can frequently furnish the necessary speed with more than adequate decontamination.

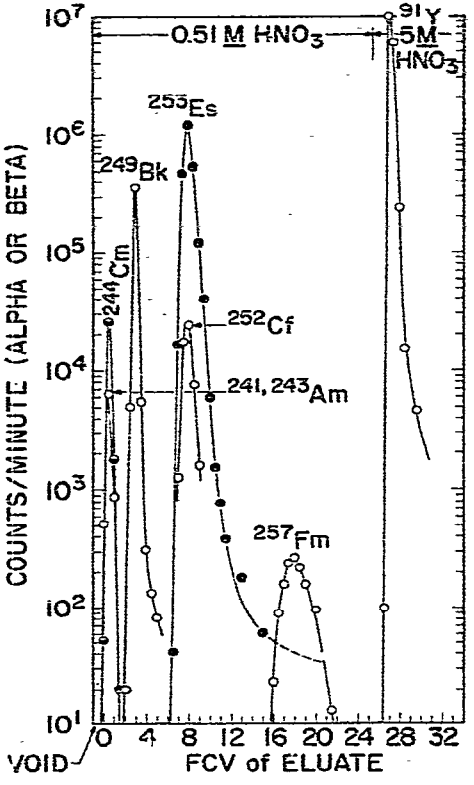

Fig. 5. Purification of $4 \cdot 10^8$ atoms of $^{257}_{100}$Fm ($t_{\frac{1}{2}} = 100$ days) using a 2-cm-long column. $T = 50°$; 25% (w/w) of 1.5 *F* HDEHP in dodecane on 5-μm Zorbax-SIL. FCV = Free column volume.

Purification of $^{257}_{100}$Fm. Fig. 5 shows the separation of $4 \cdot 10^8$ atoms (*ca.* 10^{-15} moles) of $^{257}_{100}$Fm from other transplutonium elements and from fission product yttrium. In this separation the major emphasis was on resolution and decontamination from ^{253}Es and ^{91}Y and on the recovery of the $^{257}_{100}$Fm as a weightless sample. Speed was not important; therefore, the flow velocity was optimized at *ca.* 2 cm/min in order to maximize the number of plates. A 2-cm-long column gave *ca.* 10^3 plates at the above velocity, which was sufficient to resolve not only Fm from Es but also Cm, Bk, and Es. Even the chemically similar pairs, Am–Cm and Cf–Es, were partially resolved. The decontaminations of Es and Y from Fm were *ca.* 10^4 and $>10^7$, respectively. Although the peak to tail of the Es band was between 10^4–10^5, superior shaped elution curves have been obtained with other Zorbax-SIL support (see ref. 6) and with wide-pore (350 Å) PSM support. The small column size aided in the recovery of the $^{257}_{100}$Fm as a weightless sample, and, even though speed was not

important, the entire separation required only 30 min because of the 2-cm column length.

This type of high-performance preparative radiochemical separation has many applications not only in actinide chemistry but also in the purification of other radioactive isotopes. The columns are not limited to tracer scale separations, as shown in ref. 6, and could be used at high radiation levels by increasing the flow velocity in order to minimize radiation damage.

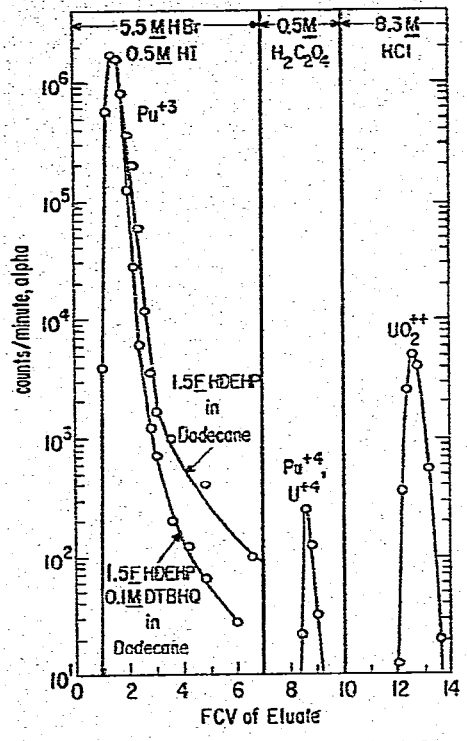

Fig. 6. Separation of U(IV) and (VI) from Pu(III) using a 5-cm-long column. $T = 25°$; 30% (w/w) of HDEHP in dodecane on 20-μm Spherisorb; $v = 2$ cm/min. FCV = Free column volume.

Measurement of $^{239}_{94}Pu$ half life. Fig. 6 shows how high-performance LLC was used to measure accurately the $^{239}_{94}Pu$ half life by quantitatively separating and recovering (99.999%) of the $^{235}_{92}U$ daughters in both the tetravalent and hexavalent oxidation states after a given period of growth. The actual measurement was performed on 1 g of $^{239}_{94}Pu$ which was reduced to the trivalent oxidation state by evaporating to dryness in concentrated hydrobromic acid. Hydroiodic acid was used as a holding reductant. The column (8 cm × 4 mm I.D.) was operated under overload conditions since Pu(III) has a $k' < 1$ in 6 M $[H^+]$. Less plutonium extracted into the stationary phase if di(*tert.*-butyl)hydroquinone (DTBHQ) was used as a holding reductant in the organic phase, although decontamination of Pu from U of $2 \cdot 10^5$ was achieved on a single column without using DTBHQ. A period of about 500 days was allowed for the growth of $^{235}_{92}U$ in an initially purified $^{239}_{94}Pu$ sample. Uranium was measured by isotopic dilution analysis after the chromatographic separation from plutonium.

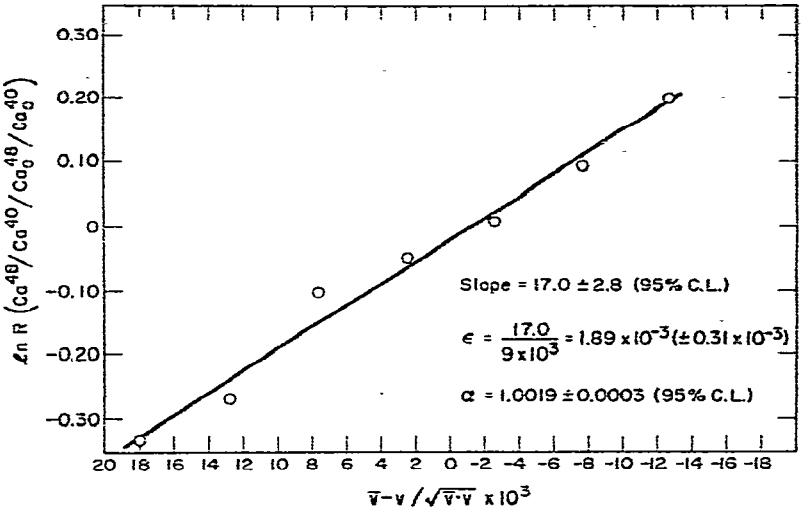

Fig. 7. Enrichment of ^{40}Ca and ^{48}Ca by high-efficiency LLC using 30% (w/w) of 1.5 *F* HDEHP in dodecane on 5-μm Zorbax-SIL. Column length = 25 cm; $T = 25°$; $k' = 6$; mobile phase = 0.044 *M* nitric acid; $v = 2$ cm/min.

The emphasis in this separation was on quantitative removal and recovery of a minor component from a major component. Both separation factors and column efficiency had to be high in order to achieve this requirement, but just as important was the minimization of channeling and tailing. This type of high-performance separation can frequently be used indirectly to make very accurate nuclear measurements.

Stable isotope separation

Because of the notable success in separating chemically similar elements using very short columns, the same high performance LLC system was extended to the problem of enriching the stable isotopes of calcium. An enrichment plot for the following isotopic exchange at 25° is shown in Fig. 7:

$$^{48}Ca_{aq}^{2+} + {}^{40}Ca(DEHP)_{2org} \rightleftarrows {}^{48}Ca(DEHP)_{2org} + {}^{40}Ca_{aq}^{2+} \quad (8)$$

The ε value for eqn. 8 is calculated from the slope of a linear least-squares fit of the data in the form shown in Fig. 7. Table IV shows the α and $\varepsilon/\Delta m$ (Δm = the dif-

TABLE IV

SEPARATION FACTOR, α, AND ε FOR CALCIUM ISOTOPES WITH THE LLC SYSTEM, HDEHP IN DODECANE–DILUTE NITRIC ACID

Stationary phase	*T* (°C)	$\varepsilon/\Delta m \cdot 10^4$ *(95% convidence level)*	α ($^{48}Ca/^{40}Ca$) *(95% convidence level)*
HDEHP–dodecane	10	3.6 ± 0.8	1.0029 ± 0.0006
	25	2.4 ± 0.4	1.0019 ± 0.0003
	50	1.5 ± 0.2	1.0012 ± 0.0002
Undiluted HDEHP	25	1.8 ± 0.2	1.0014 ± 0.0002

ference in the mass number of the isotopes) at three different temperatures and for undiluted HDEHP at 25°. Most of these data were obtained using the ^{48}Ca–^{42}Ca mixture for reasons discussed earlier. The α for $^{48}Ca/^{40}Ca$ was then calculated from $\varepsilon/\Delta m$.

The $\varepsilon/\Delta m$ is significantly larger than the $\varepsilon/\Delta m$ reported for the calcium–lactate system determined by ion-exchange chromatography[15,16]. However, the ε's are still approximately two to four times too low to achieve a practical chromatographic separation. Over 10^6 effective theoretical plates would be required to give a resolution of 0.5 and this is much too difficult to achieve even for the highest-efficiency HDEHP–Zorbax columns. It is interesting to note that the heavier isotopes of calcium are preferentially extracted by HDEHP. Aaltonen[15,17] found that the heavier isotopes of certain alkaline earths and lanthanides are preferentially complexed by α-hydroxy carboxylic acids.

In spite of the small ε, an attempt was made to enrich ^{48}Ca using a longer column. The enrichment of $^{48}Ca/^{40}Ca$ using a 75-cm-long column is shown in Table V. The 75-cm-long column was made by coupling a 50-cm column (number of plates, $N = 20{,}000$) and a 25-cm column ($N = 10{,}000$). An optimum flow velocity of $v = 2$ cm/min was selected from the H *vs.* v curve shown in Fig. 3. (The H *vs.* v curve clearly shows the futility of trying to achieve greater column efficiency by reducing the flow velocity below 1 cm/min, as is sometimes done[16], because at these low velocities the longitudinal diffusion effect becomes important.) Three different cut points were taken in order to show the increase in ^{48}Ca enrichment in the latter half of the band. The data in Table V do show a definite enrichment of the heavy isotope, although it is not sufficient to be of any practical importance. (The enrichment and composition data in Table V are the integrated values from the cut point to the last 1% of the elution band.)

TABLE V

ENRICHMENT OF $^{48}Ca/^{40}Ca$

Column length = 75 cm; $v = 2$ cm/min; $k' = 6$ (25°) and 8 (9°); stationary phase, 25% (w/w) of 1.5 *F* HDEHP in dodecane on 5 μm Zorbax-SIL.

T (°C)	*Cut point (%)*	*Enrichment*	*Composition (%)*	
25	50	1.06	49	51
25	25	1.14	47	53
25	10	1.31	43	57
9	50	1.05	49	51
9	25	1.10	48	52
9	10	1.15	46	54

Since α is larger at lower temperatures, an attempt was made to improve the ^{48}Ca enrichment by eluting the calcium at 9°. However, the data in Table V show essentially the same results as obtained at 25°. This may be explained by the substantial loss in column efficiency at the lower temperature (owing primarily to slow interfacial mass transfer) as shown in the H *vs.* v curve in Fig. 3. The low-temperature data indicate that α at 9° is 1.0024, which is within the experimental error given in Table IV. Although column efficiency is highest at 50°, α is lower, and

thus no substantial advantage would be gained by eluting the calcium at this temperature.

ACKNOWLEDGEMENTS

The authors wish to thank Dr. J. J. Kirkland of the Central Research and Development Department, E. I. duPont de Nemours & Co., Inc., for supplying the wide-pore PSM material and for his helpful discussions. We also thank Mr. Donald J. Rokop and Mrs. Alice M. Essling for performing the very difficult mass spectrometric analyses, and Mr. Herbert Diamond for performing the ^{239}Pu half life measurements.

REFERENCES

1 T. Braun and G. Ghersini (Editors), *Extraction Chromatography*, Elsevier, Amsterdam, Oxford, New York, 1975.
2 E. P. Horwitz and C. A. A. Bloomquist, *J. Inorg. Nucl. Chem.*, 34 (1973) 385.
3 E. P. Horwitz and C. A. A. Bloomquist, *J. Inorg. Nucl. Chem.*, 35 (1973) 271.
4 E. P. Horwitz and C. A. A. Bloomquist, *J. Chromatogr. Sci.*, 12 (1974) 11.
5 E. P. Horwitz and C. A. A. Bloomquist, *J. Chromatogr. Sci.*, 12 (1974) 200.
6 E. P. Horwitz, C. A. A. Bloomquist and W. H. Delphin, *J. Chromatogr. Sci.*, in press.
7 E. P. Horwitz and C. A. A. Bloomquist, *J. Inorg. Nucl. Chem.*, 37 (1975) 425.
8 E. Glueckauf, *Trans. Faraday Soc.*, 54 (1958) 1203.
9 J. C. Giddings, *Dynamics of Chromatography, Part I, Principles and Theory*, Marcel Dekker, New York, 1965, Ch. 3, p. 95.
10 G. F. Vandegrift and E. P. Horwitz, *J. Inorg. Nucl. Chem.*, in press.
11 G. C. Lowrison, *Crushing and Grinding*, Butterworths, London, 1974, Ch. 2, p. 8.
12 J. C. Giddings, *Dynamics of Chromatography, Part I, Principles and Theory*, Marcel Dekker, New York, 1965, Ch. 4, p. 166.
13 R. F. Nolte, S. Specht and H.-J. Born, *J. Chromatogr.*, 110 (1975) 239.
14 S. Specht, R. F. Nolte and H.-J. Born, *J. Chromatogr.*, 110 (1975) 253.
15 J. Aaltonen, *Suom. Kemistil. B*, 44 (1971) 1.
16 D. A. Lee, *J. Inorg. Nucl. Chem.*, 38 (1976) 161.
17 J. Aaltonen, *Ann. Acad. Sci. Fenn., Ser. A*, 11 (1967) 137.